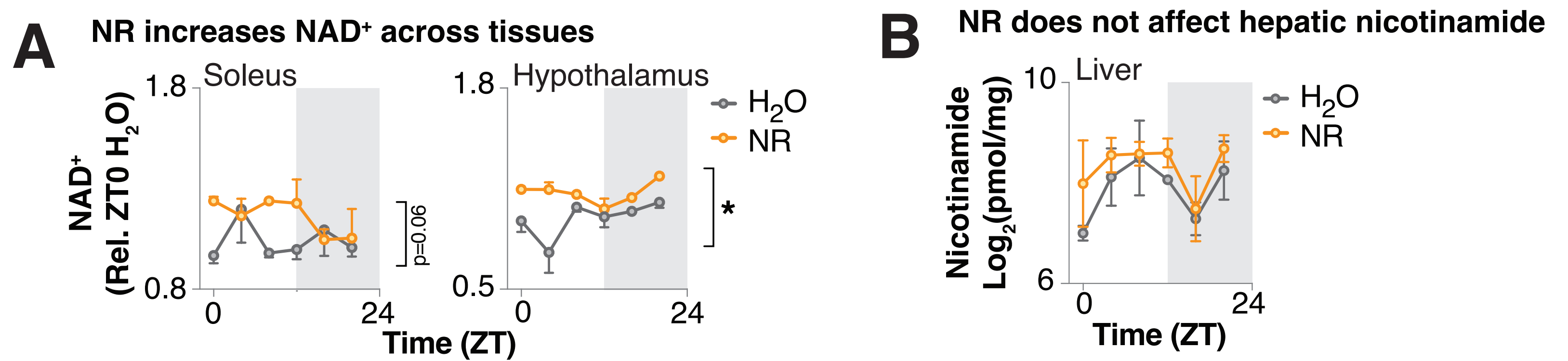

C **Similar proportion, distribution, and characteristics of reprogrammed genes with 5% FDR cutoffs**

NR

554
486
346
1819

Loss | Phase-shift | Gain | Unaffected

Loss genes | **Gain genes** | **Phase-shift genes** (H_2O, NR)

0 | 6 | 12 | 18

Loss genes

		Rank	Term	-logP
Promoter Motifs:	2-8	1	ETS	11.15
	2-8	8	Forkhead	6.46
	16-18	1	GATA	5.36
	16-18	5	Zn-Finger	4.53
Gene Ontology:	2-8	1	Rib. euks	13.43
	2-8	2	Spliceosome	12.31
	16-18	1	ErbB sig.	5.45
	16-18	3	Insulin sig.	4.10

Gain genes

		Rank	Term	-logP
Promoter Motifs:	2-8	1	PAX	5.69
	2-8	9	HOX	3.99
	16-18	1	ETS	6.56
	16-18	5	STAT	4.64
Gene Ontology:	2-8	1	Paths cancer	5.15
	2-8	2	Vit. D3 biosyn.	4.26
	16-18	1	Rib. biogen.	9.57
	16-18	3	Spliceosome	7.54

Phase-shift genes

		Rank	Term	-logP
Promoter Motifs:	16-22	1	ETS	6.56
	16-22	5	HSF	4.64
Gene Ontology:	16-22	1	Spliceosome	10.13
	16-22	3	Ribosome	7.80

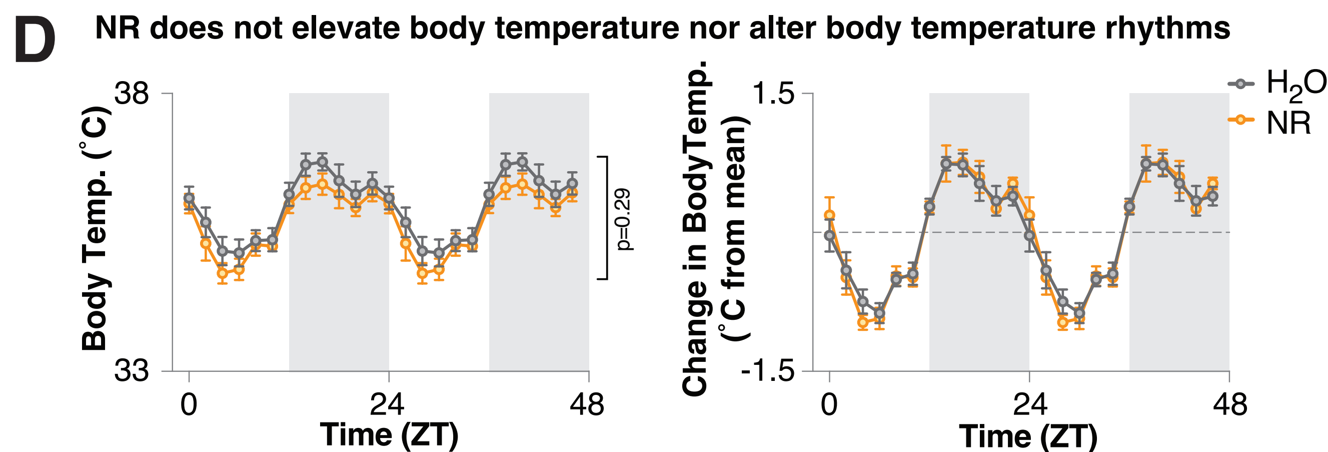

E **NMN supplementation elevates hepatic NAD⁺ in WT and *Bmal1⁻/⁻* mice (ZT6)**

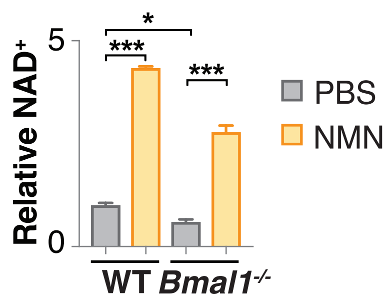

Figure S1. Nicotinamide riboside (NR) and nicotinamide mononucleotide (NMN) supplementation elevates NAD^+ across tissues without changing body temperature. Related to Figures 1-4. **(A)** NAD^+ quantified by HPLC from soleus and hypothalamus from 8 month old mice that had access to NR-supplemented drinking water for 4 months (*$p<0.05$ ANOVA). **(B)** Hepatic nicotinamide quantified by LC-MS. **(C)** eJTK- Cycle analysis following RNA-seq every 4 hrs across the 24-hr day identified transcripts that lost, gained, phase-shifted >4 hrs oscillations, or were unaffected following NR with FDR-adjusted p-values of <0.05 and >0.95 for cycling and non-cycling genes, respectively. Pie chart shows total genes within each group (left, top), radial histograms show number of genes whose oscillations peak within each 2-hr window, with the radius corresponding to 100 genes (right, top). Dark gray shading on radial histograms indicates the groups of genes within each reprogramming group that are subjected to promoter motif and gene ontology analysis for which select terms ranked in the top 10 are shown (bottom). **(D)** Body temperature rhythms measured every 2 hrs for 24 hrs (double plotted for clarity) in either NR- or H_2O-treated 9.5 mo old WT mice (n=6-8). Left panel shows raw body temperature (˚C) while right panel shows change in body temperature from the average body temperature. **(E)** Quantification of hepatic NAD^+ (ZT6) by HPLC in WT and *Bmal1*$^{-/-}$ mice injected with either saline or NMN (i.p. 500 mg/kg) at ZT2 (*$p<0.05$, ***$p<0.001$).

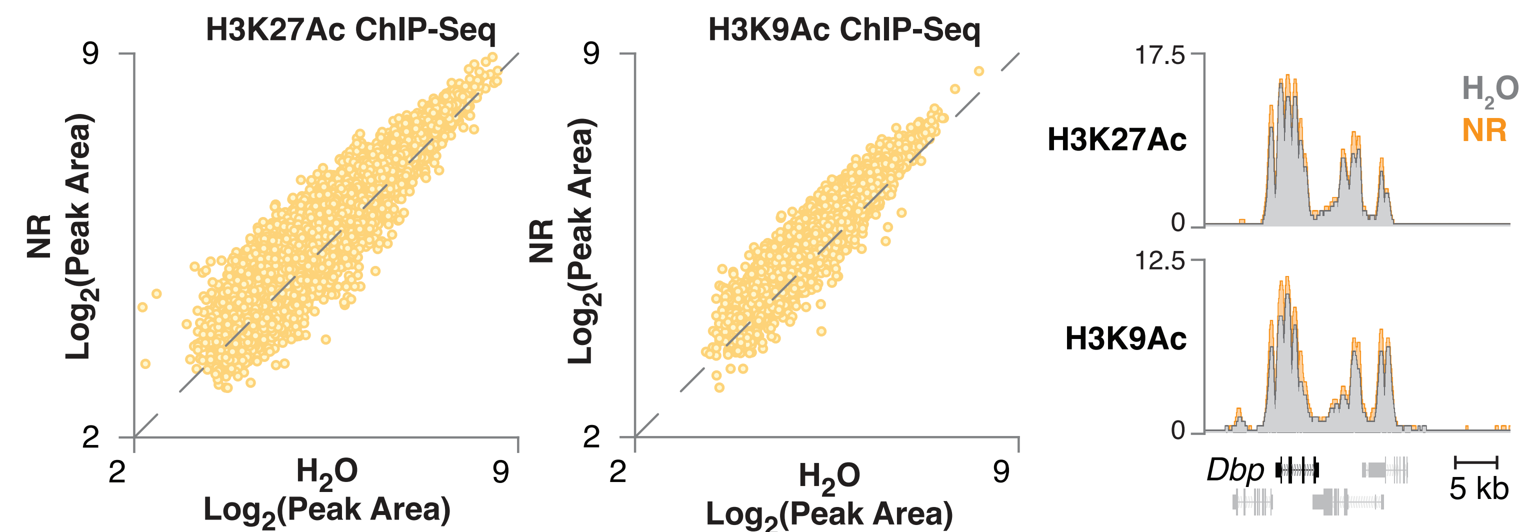
A
NR increases acetylation of H3K27 and H3K9 genome-wide and at the Dbp locus (ZT8)
H3K27Ac ChIP-Seq
H3K9Ac ChIP-Seq
NR
Log2(Peak Area)
H2O
Log2(Peak Area)
9
2
17.5
12.5
0
H3K27Ac
H3K9Ac
H2O
NR
Dbp
5 kb

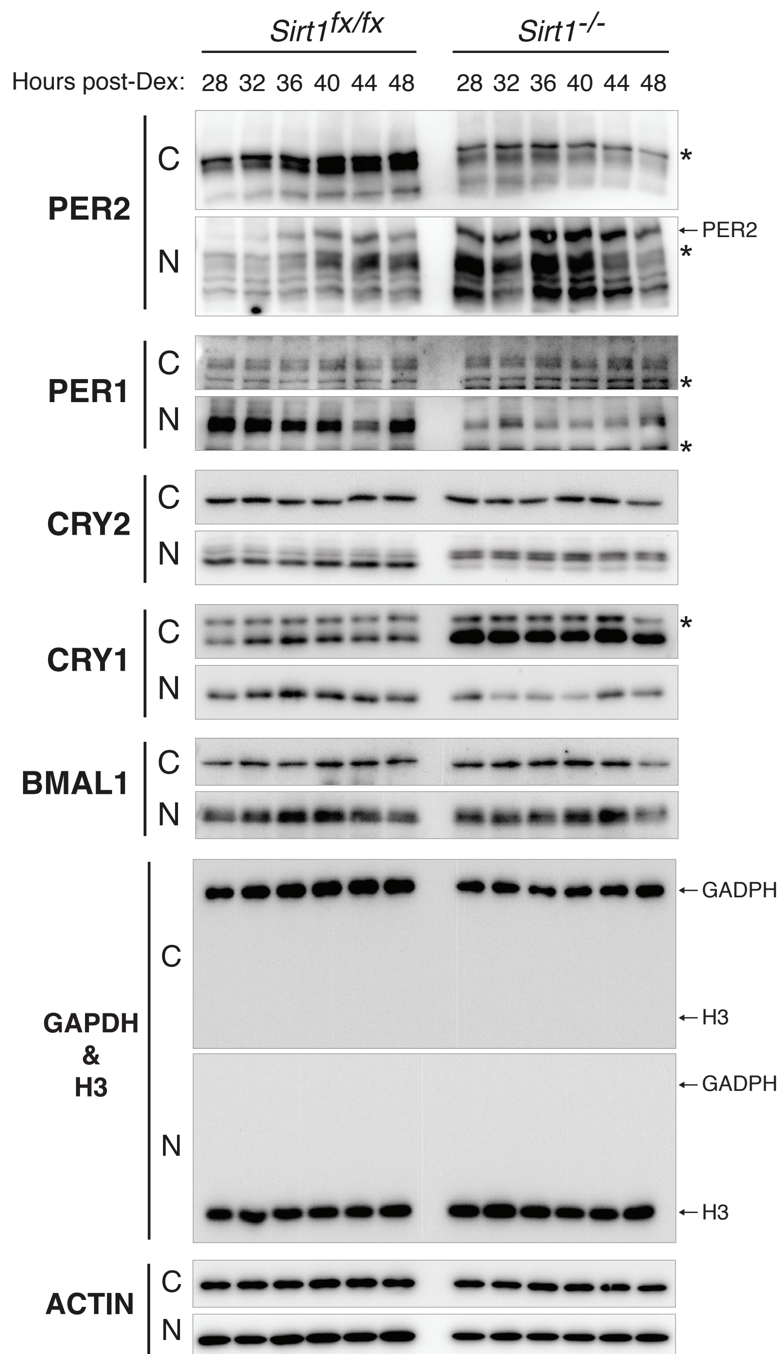
B
Subcellular fractionation in Sirt1-/- MEFs
Sirt1fx/fx
Sirt1-/-
Hours post-Dex: 28 32 36 40 44 48 28 32 36 40 44 48
PER2
PER1
CRY2
CRY1
BMAL1
GAPDH
&
H3
ACTIN
C
N
*
PER2
GADPH
H3

Figure S2. SIRT1 is required for increased chromatin recruitment of BMAL1 following NMN supplementation and for proper clock repressor subcellular localization. Related to Figure 5. **(A)** ChIP-seq for H3K27Ac and H3K9Ac in liver (ZT8) following 6 months of NR-supplementation compared to H_2O. Scatter plots depict average log-transformed tag densities for all H3K27Ac and H3K9Ac peaks (n=2). UCSC genome browser images of average H3K27Ac and H3K9Ac tag density at the *Dbp* locus in liver during H_2O or NR supplementation. Maximum track height is indicated on the y-axis, and gene orientation is indicated below. **(B)** Western blots of clock proteins from cytoplasmic (C) and nuclear (N) fractionated dexamethasone-synchronized *Sirt1*$_{fx/fx}$ and *Sirt1*$_{-/-}$ MEFs. An equimolar mix of GAPDH and H3 antibodies was used to validate subcellular fractionation. Asterisks indicate non-specific bands.

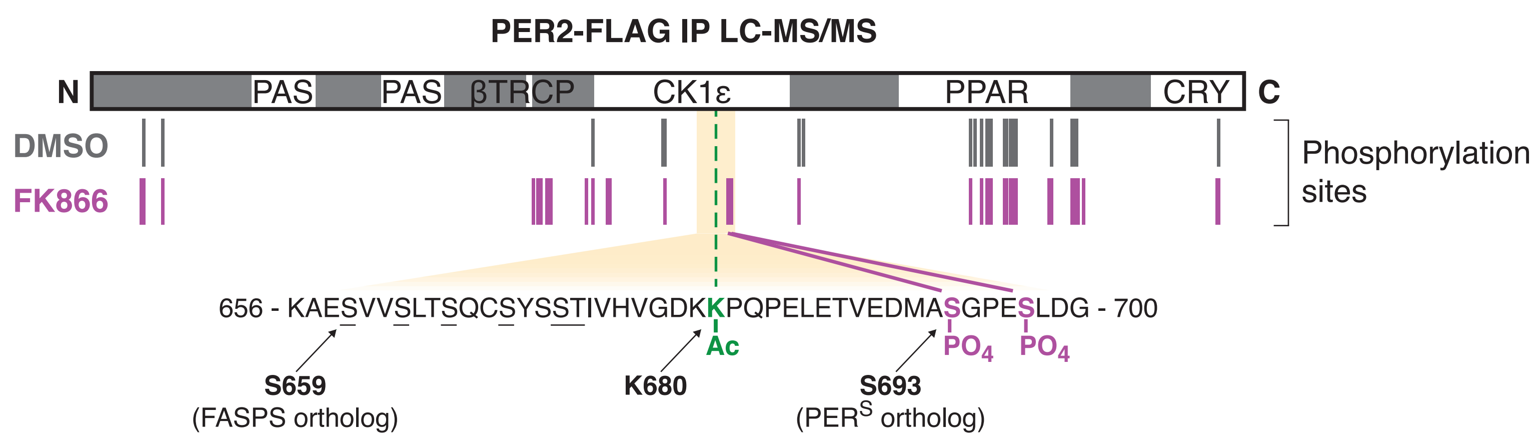

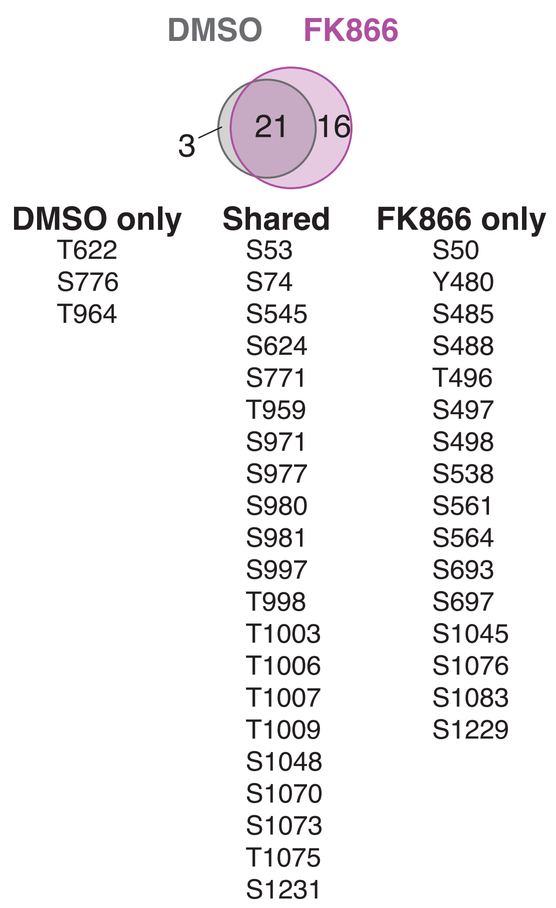

DMSO only	Shared	FK866 only
T622	S53	S50
S776	S74	Y480
T964	S545	S485
	S624	S488
	S771	T496
	T959	S497
	S971	S498
	S977	S538
	S980	S561
	S981	S564
	S997	S693
	T998	S697
	T1003	S1045
	T1006	S1076
	T1007	S1083
	T1009	S1229
	S1048	
	S1070	
	S1073	
	T1075	
	S1231	

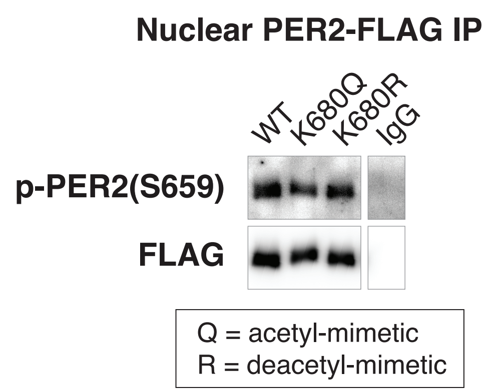

Figure S3. Pharmacologic inhibition of NAD+ biosynthesis controls post-translational modification of PER2. Related to Figure 5. (A-B) LC-MS/MS identification of phospho-modifications on PER2 in at least 3 out of 4 replicates treated with DMSO (gray) or FK866 (purple). K680-proximal regions are annotated for previously identified FASPS-associated phosphorylation sites (underlines) and orthologous sites in human and *Drosophila*. (**C**) Western blot analysis of phospho-PER2(S659) following PER2-FLAG immunoprecipitation from HEK293 cells expressing WT, acetyl-mimetic (K680Q), or de-acetyl-mimetic (K680R) PER2. The IgG sample was run on the same gel as the other samples shown.

A Decreased NAD^+ in old mice restored by NR (ZT0) without affecting weight

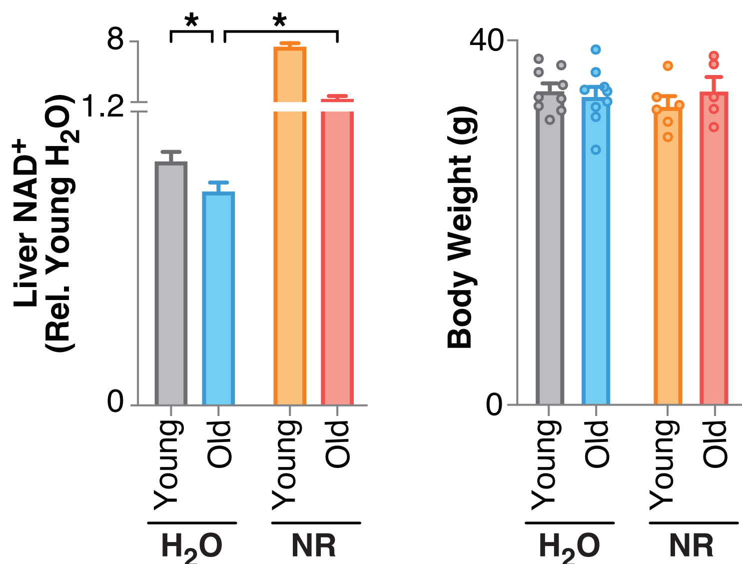

D NR restores HSF1 chromatin binding in old mice

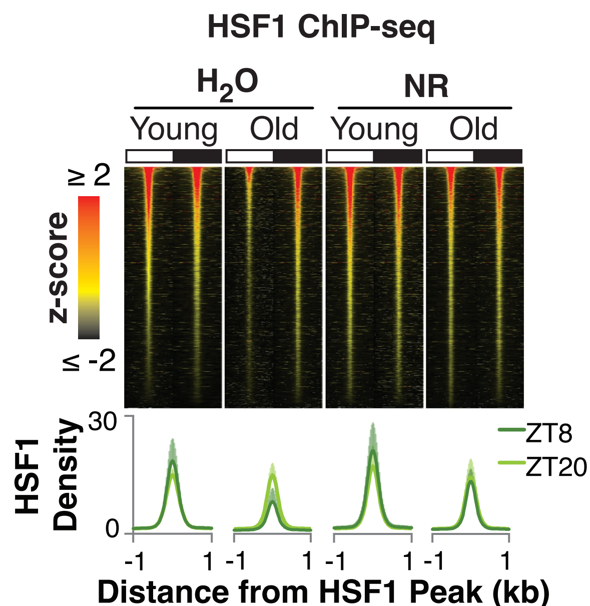

B NR restores BMAL1 chromatin occupancy at *Per2* promoter in old mice

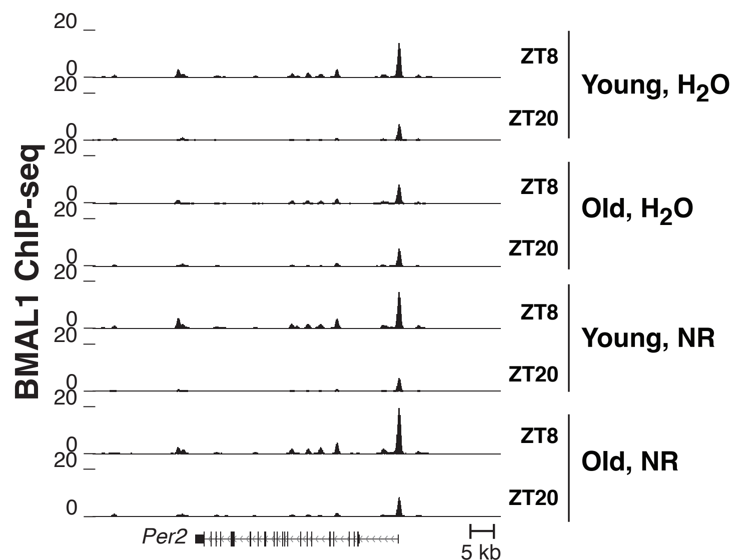

E *Nampt* ablation decreases late-night activity

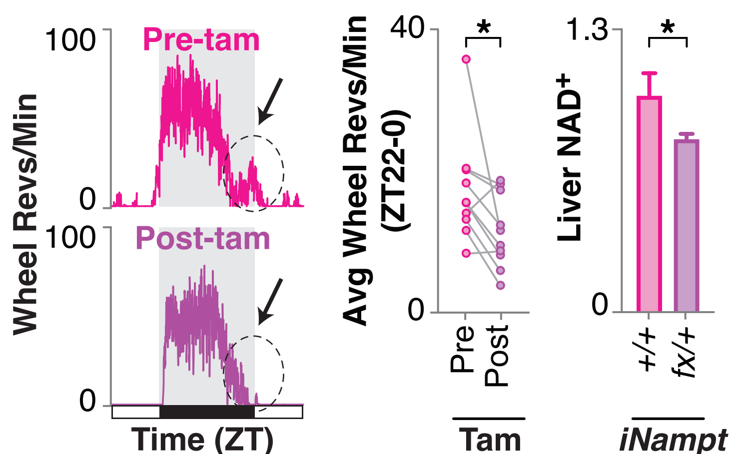

C NR restores BMAL1 chromatin binding at metabolic genes and those containing Rossman-fold protein structure

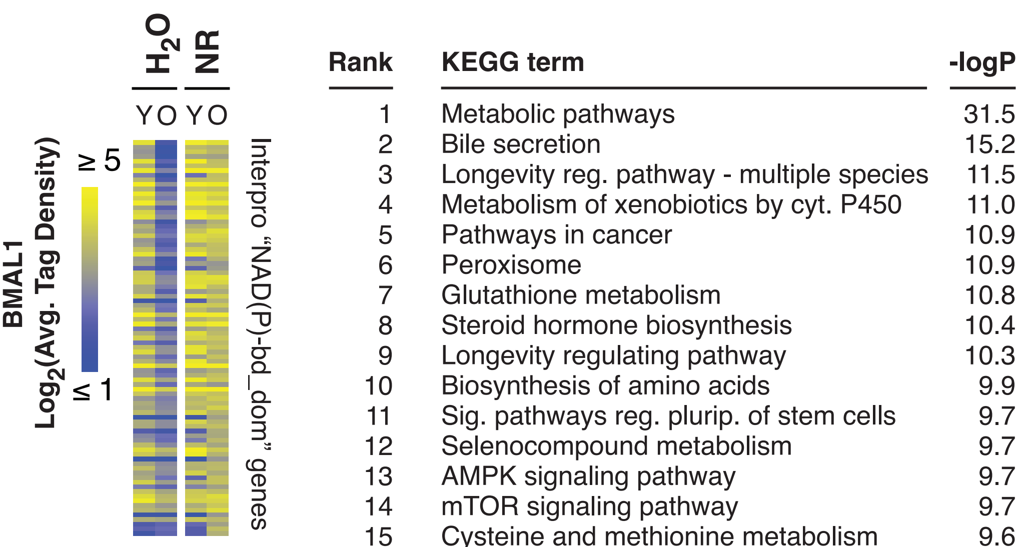

Rank	KEGG term	-logP
1	Metabolic pathways	31.5
2	Bile secretion	15.2
3	Longevity reg. pathway - multiple species	11.5
4	Metabolism of xenobiotics by cyt. P450	11.0
5	Pathways in cancer	10.9
6	Peroxisome	10.9
7	Glutathione metabolism	10.8
8	Steroid hormone biosynthesis	10.4
9	Longevity regulating pathway	10.3
10	Biosynthesis of amino acids	9.9
11	Sig. pathways reg. plurip. of stem cells	9.7
12	Selenocompound metabolism	9.7
13	AMPK signaling pathway	9.7
14	mTOR signaling pathway	9.7
15	Cysteine and methionine metabolism	9.6

Figure S4. NAD$^+$ repletion through NR supplementation restores circadian rhythms of stress and metabolic transcription during aging. Related to Figure 6. (A) Liver NAD$^+$ quantified by HPLC in young (10 mo) and old (22 mo) *Per2::Luciferase* mice at ZT0 following 6 mo of NR-supplemented or regular drinking water (*p<0.05) (n=6). Body weights of young and old WT mice that were treated with NR-supplemented or regular drinking water for 6 months were weighed prior to collection. **(B)** UCSC tracks depicting average BMAL1 ChIP-seq signal proximal to *Per2* in liver (ZT8 and ZT20) of young and old mice treated with H_2O or NR. **(C)** Gene ontology for genes that are proximal to BMAL1 peaks found in old mice treated with NR, but absent in old mice treated with H_2O (HOMER). (*left*) Top 15-enriched KEGG gene ontology terms. (*right*) Heat map of average ZT8 BMAL1 tag-densities that annotate to genes that express proteins with the Rossman-fold NAD$^+$-binding domain (Top-enriching Interpro gene ontology term: IPR016040, -logP = 16.9). **(D)** HSF1 ChIP-seq in liver (ZT8 and ZT20). Z-score normalized average tag-densities for genomic regions corresponding to the center of each HSF1 peak identified in old mice treated with NR ± 1 kb and sorted by size (n=2) (*Bottom*) Average HSF1 tag-density and standard error for both replicates within each group. **(E)** (*Left*) Average daily profile of *ad lib* wheel running activity in inducible *CAG^{CreER}; Nampt$^{fx/+}$* mice before and after tamoxifen. Arrow denotes 'late-night activity'. (*Middle*) Quantification of average wheel revolutions/min in the late night (ZT22-0) (n=10) (*p<0.05). (*Right*) Hepatic NAD$^+$ quantified by HPLC at ZT0 following tamoxifen administration to *CAG^{CreER}; Nampt$^{fx/+}$* or *CAG^{CreER}; Nampt$^{+/+}$* mice (n=3-8. * p<0.05).